Structural Engineering and Mechanics, *Vol. 69, No. 6 (2019) 651-665*
DOI: https://doi.org/10.12989/sem.2019.69.6.651

The length of plastic hinge area in the flanged reinforced concrete shear walls subjected to earthquake ground motions

Farzad Ghaderi Bafti[1a], Alireza Mortezaei[*1] and Ali Kheyroddin[2b]

[1]*Civil Engineering Department, Seismic Geotechnical and High Performance Concrete Research Centre, Semnan Branch, Islamic Azad University, Semnan, Iran*
[2]*Civil Engineering Faculty, Semnan University, Semnan, Iran*

(Received December 8, 2018, Revised January 30, 2019, Accepted February 5, 2019)

Abstract. Past earthquakes have shown that appropriately designed and detailed buildings with shear walls have great performance such a way that a considerable portion of inelastic energy dissipation occurs in these structural elements. A plastic hinge is fundamentally an energy diminishing means which decrease seismic input energy through the inelastic deformation. Plastic hinge development in a RC shear wall in the areas which have plastic behavior depends on the ground motions characteristics as well as shear wall details. One of the most generally used forms of structural walls is flanged RC wall. Because of the flanges, these types of shear walls have large in-plane and out-of-plane stiffness and develop high shear stresses. Hence, the purpose of this paper is to evaluate the main characteristics of these structural components and provide a more comprehensive expression of plastic hinge length in the application of performance-based seismic design method and promote the development of seismic design codes for shear walls. In this regard, the effects of axial load level, wall height, wall web and flange length, as well as various features of earthquakes, are examined numerically by finite element methods and the outcomes are compared with consistent experimental data. Based on the results, a new expression is developed which can be utilized to determine the length of plastic hinge area in the flanged RC shear walls.

Keywords: plastic hinge; flanged shear wall; time history analysis; RC element

1. Introduction

Past earthquakes in various earthquake prone areas like Iran, Japan, USA and New Zealand have shown that the reinforced concrete structures in the countries with high seismicity may be vulnerable to the moderate to severe damages. Hence, a properly selected structural system is essential for a good performance under the seismic loading. Reinforced concrete shear wall system has been accepted as an effective lateral load bearing system to improve the performance and integrity of the RC buildings under the dynamic forces such as tectonic earthquakes. As can be seen in Fig. 1, shear walls usually have rectangular section. When RC columns are provided at either ends of the wall, termed as boundary elements, a barbell shape results. The flanged wall sections are created when the intersecting walls exist.

The usefulness of flanged RC structural walls in the structural planning of medium- and high-rise buildings has been widely recognized. When the structural walls are situated in suitable positions, they can be very efficient in resisting lateral loads against strong ground motions. Aside from the potential stiffness and strength those flanged shear walls possess and enable them to carry large lateral loads, they offer considerable ductility. It means that shear walls provide a potentially high-ductile system with a sought degree of redundancy. On the other hand, designers usually tend to concentrate the structural walls around staircase and elevator cores to reduce interactions with the story plan and to take full advantage of accessible space. Accordingly, linear structural walls in rectangular form are merged regularly to shape T-, C-, I- and L-forms.

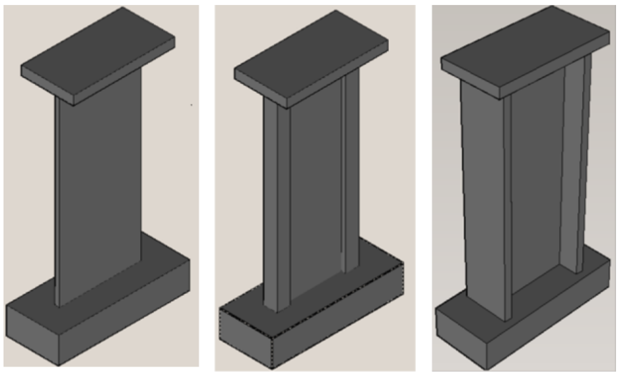

Fig. 1 Different types of shear wall cross section

As it was well clarified by ACI 318-14 (ACI Committee 318 2014), in the dual system buildings, shear walls are the first and major seismic parts resisting to earthquake actions. They are designed relying on capacity design principles

*Corresponding author, Associate Professor
E-mail: a.mortezaei@semnaniau.ac.ir
[a]Ph.D. Candidate
[b]Professor

Copyright © 2019 Techno-Press, Ltd.
http://www.techno-press.com/journals/sem&subpage=7
ISSN: 1225-4568 (Print), 1598-6217 (Online)

while moment resisting frames are considered as secondary seismic parts. For this reason, a key part of the seismic design of concrete wall buildings is ensuring which the flexural displacement capacity of the walls is higher than the demand of flexural displacement.

Plastic hinge model has been widely used in seismic design codes to evaluate deformation capacity of RC structural walls. With the development of performance/displacement based seismic design, designers are required to go beyond code prescriptions and accurately predict how a structure will respond to extreme events. Accurate assessment of the plastic hinge length has an importance role in connecting the displacement ductility of RC shear walls to the section curvatures. Various methods and models have been recommended in the past to examine the nonlinear behavior of this area for accurately estimating the RC shear wall ductility. For instance, relying on the beam specimens tests, it is a routine practice in a RC structural wall to assume that the length of plastic hinge area, l_p, varies from 0.5 to 1.0 times the wall length l_w. Wall length is defined as larger horizontal width of the structural wall. Hence, for safe estimating of curvature and displacement capacity $0.5l_w$ is considered as a lower-bound estimation of plastic hinge. However, due to the significance of plastic hinge characteristics in estimating the ductility of RC shear walls and for the sake of intricacy and nonlinearity engaged in this mechanism, large discrepancies exist for estimation of plastic hinge length. On the other hand and owing to the importance of the topic, an accurate expression for plastic hinge length of flanged shear walls is needed more than ever.

Furthermore, it is usually supposed that areas of a structural wall outside the selected plastic area can be simulated with elastic models. Nevertheless, in high-rise and slender structural walls, seismic demands at the hazard level of Maximum Credible Earthquake (MCE) depend on nonlinear behavior, which could lead to large amplifications in flexural moment and shear force compared to outcomes resulted from elastic behavior. To make these predictions often requires a widespread examination review of the shear wall and also some essential parameters such as plastic hinge length. The length of plastic hinge area in the flanged RC walls has been less considered and studied. There are few studies in this regard.

Hereupon, the present study was conducted with the aim of founding a simple and practical relationship for the length of plastic hinge area in flanged RC shear walls utilizing over 1020 inelastic time-history analyses. In the next sections, primarily, a number of methods and models to determine the length of plastic hinge area in RC components are defined. Literature review, specifications of selected earthquake records, parametric studies, suggested simple equation and concluding remarks are mentioned later. The outcomes are accounted for here.

2. Plastic hinge area

The occurrence of inelastic action in many structural RC walls during strong earthquakes is evident in the observations made thus far. Extensive experimentation has been accomplished to assess the behavior of rectangular RC walls, particularly plastic hinge length, under the monotonic and cyclic loading. The results have been used in arriving at appropriate design and detailing provisions in the building design codes.

Plastic hinges are the development of ductile design theory in earthquake-resistant building structures. The seismic energy is dissipated through the plastic deformation of particular areas at the end of a member without any failure in the rest of the structure. The length of plastic hinge area has a key role in seismic rehabilitation of old buildings as well as design of new structures. As the characteristics of plastic hinge area are narrowly connected to the seismic behavior of concrete components, it must be examined accurately to avoid failure during seismic incidences.

This region involves the areas of reinforcement yielding, concrete crushing and curvature positioning. Once, the entire cross section has yielded, it is said to be “plastic”. The areas of plastic hinge are usually generated at the segments of maximum moment and cause changes in the curve of elastic moment. There are several procedures and methods for determining the length of plastic hinge area in a concrete member which are divided into two general categories: analytical method and experimental method. Since the emphasis and evaluation basis of this paper is on the analytical method, this method is described below.

2.1 Analytical method

For determining and evaluating the characteristics of plastic hinge area in RC members, the analytical method is based on the moment-curvature analysis. Moment-curvature analysis is a precise method for determining the load deformation behavior of a concrete cross section using nonlinear material properties.

Relying on the existing standards (EN 1992-1-1 2004, CSA A23.3-14 2014, ASCE/SEI 7-16 2017, ASCE/SEI 41-17 2017), nonlinear methods should be used to assess the bearing capacity of structural shear walls under the seismic loads. In order to obtain a more precise simulation regarding the actual structural behaviour, designers need supplementary information including moment-curvature curve. Therefore, the exact determination of relationship between flexural bending and cross-section curvature as moment-curvature diagram in concrete sections is a suitable and reliable index for determining the bearing capacity of structures under the seismic loading (Mortezaei and Ronagh 2012). For a concrete cross section with given structural characteristics, depending on the required accuracy, moment-curvature relationship curve is available in actual or idealized form (Fig. 2). Moment-curvature relationship curves are usually described by three characteristic points which represent three different structural states.

The first characteristic point is to obtain the tensile strength at the farthest tensile fibre of concrete cross section ($M=M_{cr}$). When the concrete reaches its tensile strength, a crack appears in the section (M_{cr} and ϕ_{cr}). The crack propagates with increasing tensile load, which leads to a decrease in moment-inertia of cross section. The next point is yielding mode occurrence in the tensile steel

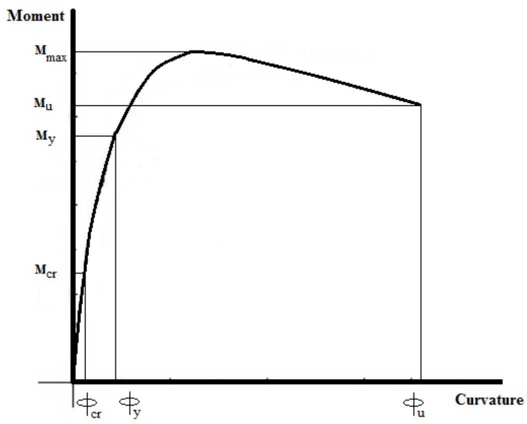

(a)

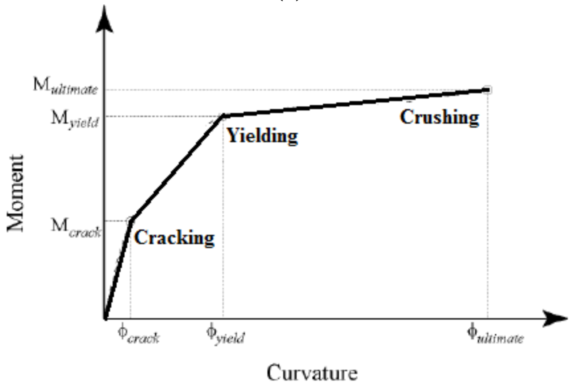

(b)

Fig. 2 Moment-curvature relationship curve in (a) actual and (b) idealized form

reinforcements (M=M_y). At this stage, simultaneously with the tensile steel yielding, the concrete cover starts to crush and the failure mode begins with the formation of plastic hinge in the base of structural wall. The third point is the collapse point which followed by crushing the core concrete, buckling the longitudinal reinforcements, and failure of the transverse reinforcements. This stage can be terminated by collapse of tensile steel reinforcements or failure of compressive concrete.

In determining the rotational capacity of concrete members, the section curvature as well as curvature distribution throughout the member is considered. Based on the principles of mechanics of material, the quantity of rotation between two points (p and q) is equal to the area below the curvature curve between these two points. That means

$$\theta_{pq} = \int_p^q \phi \, dx \tag{1}$$

Before steel reinforcement yielding, curvature is distributed more evenly over the structural wall. Following yielding the tensile rebars, the amount of curvature in the basement regions of the shear wall is rapidly increased and the plastic curvature is concentrated in certain areas of the wall. There is a border point (ϕ_y) from which the amount of wall curvature increases sharply to the wall base after

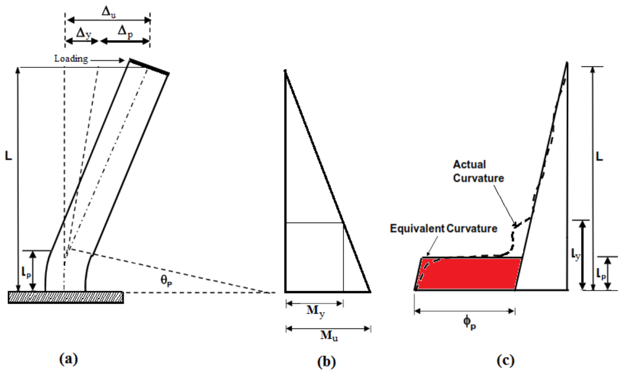

Fig. 3 Curvature distribution and lateral deformation across a structural wall: (a) RC shear wall, (b) moment diagram, (c) curvature curve

yielding, while outside this area, from this point to the wall tip, the amount of curvature remains almost unchanged. This area from the wall base to the border point is called yielding length (l_y). With respect to the Eq. (1), plastic rotation (θ_p) can be determined by following equation

$$\theta_p = \int_0^{l_y} \left| \phi(x) - \phi_y \right| dx \tag{2}$$

The plastic rotation can be obtained by computing the shaded area in Fig. 3 as well as the area of equivalent block.

$$\theta_p = (\phi_u - \phi_y)\, l_p = \int_0^{l_y} \left| \phi(x) - \phi_y \right| dx \tag{3}$$

In which ϕ_u and ϕ_y are the amount of curvatures at the ultimate and yield load, respectively, and l_p is the equivalent length of the plastic hinge area over which the plastic curvature is supposed to be constant (Fig. 3).

$$l_p = \frac{\theta_p}{\left(\phi_u - \phi_y\right)} = \frac{\theta_p}{\phi_p} \tag{4}$$

Therefore, the equivalent length of plastic hinge area is obtained by multiplying the yielding length (l_y) in a dimensionless coefficient (α), called shape factor or curvature distribution coefficient, which is smaller than one ($l_p = \alpha . l_y$).

2.2 Former research works

Since determining the length of plastic hinge area is a fundamental step in estimating the residual deformation and load-displacement response of concrete components, many researchers have examined and criticized it. Moreover, the necessity of intense confinement in plastic hinge region to increase the ductility of reinforced concrete members as well as structural stability under the severe earthquakes has attracted the attention of many codes and guidelines. In accomplished studies regarding the length of plastic hinge area, most of the past research works have been related to the skeletal structural elements, i.e., beams and columns.

Compared to these structural components, fewer studies have been done on the characteristics of plastic hinge area in structural shear walls, especially flanged shear walls. Here, some of the earlier well-known proposed equations for RC shear walls are presented in two sections of experimental and analytical research works.

3. Experimental works

Oesterle *et al.* (1984) conducted tests of isolated reinforced concrete structural walls subjected to inelastic load reversals to study their web crushing strength. In this study, they considered a length of plastic hinge equal to the horizontal length of the wall section, l_w.

Paulay and Priestly (1993) reported tests on ductile concrete walls of rectangular shape subjected to seismic loading to study out-of-plane buckling. In this study, they used the following expression to estimate the length of plastic hinge area

$$L_p = 0.2 l_w + 0.044 H_w \tag{5}$$

Where H_w is the total height of the wall and l_w is wall length. The authors indicated that above equation predicts conservatively the plastic hinge, so that the curvature ductility demands are not underestimated; and that it gives a good approximation of the portion of the height of the wall over which out-of-plane buckling can occur.

Panagiotakos and Fardis (2001) reported tests on 61 specimens were representative of walls with rectangular and barbell sections. Walls with and without confined boundaries were tested. They were subjected to monotonic and cyclic loading. The tests continued until failure. The results were used to arrive for expressions for the plastic length that provided the best fit to these data. They developed the following expressions to determine the length of plastic hinge area:

For cyclic loading

$$L_{p,cy} = 0.12 L_s + 0.014 a_{sl} d_b f_y$$

For monotonic loading

$$L_{p,mon} = 1.5 L_{p,cy} = 0.18 L_s + 0.021 a_{sl} d_b f_y \tag{6}$$

where

$L_{p,cy}$: Plastic hinge length for cyclic loading.

$L_{p,mon}$: Plastic hinge length for monotonic loading.

a_{sl}: Zero-one variable. It is equal to one if slippage of the longitudinal reinforcement is possible and zero if it is not possible.

f_y: Yield stress of the tension reinforcement, in MPa.

Thomsen and Wallace (2004) conducted tests of slender reinforced concrete walls with rectangular shaped and T-shaped cross section with adequate quantities of transverse reinforcement in the boundary elements. They reported the results obtained for four walls. The four wall specimens included two with rectangular sections and two with T-sections. The wall samples were subjected to cyclic lateral displacements applied at the top, and a constant compressive axial load. The authors showed that plastic hinge length had a very significant influence on the strain profile. They compared the experimental and analytical strain profiles, considering plastic hinge lengths of $0.33l_w$, $0.5l_w$ and $0.67l_w$; and determined that plastic hinge lengths between o.33l_w and $0.5l_w$ produced the best agreement between results.

Preti and Giuriani (2011) conducted an experimental research work regarding the ductility of RC shear walls in the mid-rise building structures. A five-story RC shear wall in actual size was examined to get the results without influencing the size effect phenomenon. To avoid early rebar fracture and shear sliding of the wall web, a special detailing with large diameter longitudinal rebars was utilized. Cyclic loads of increasing amplitude were applied under the displacement control. A drift of 2.5% was reached without strength degradation. At this large value of drift, the test was stopped to avoid non repairable damage. The results showed that the extension of the plastic region increased together with the drift value. At 2.5% drift, its value was about 110% of the wall cross-section length.

Six shear wall specimens were tested by Christidis *et al*. (2013) under the static cyclic loading. The purpose of this research work was assessing the behaviour of concrete shear walls which do not conform to modern seismic codes, i.e., Eurocode 2 (EC2) and Eurocode 8 (EC8). The results showed that the shear walls without seismic detailing develop lower levels of ductility. The reduction of ductility level was more significant in the walls with low shear reinforcement ratio. Also, the presence of confined boundary flange elements can increase the deformation capacity of shear walls.

Mehmood *et al*. (2015) conducted an experimental program including a large-scale RC shear wall specimen with an aspect ratio of 2. In this work, a full-scale flexure-shear dominated reinforced concrete shear wall was tested under the reversed cyclic quasi-static loading. The results showed that low confinement reinforcement in the boundary elements cause buckling of longitudinal reinforcement. Moreover, a severe coupling effect was observed in flexure and shear responses which affect the length of plastic hinge area.

A study on the nonlinear behaviour of a shear wall was carried out by Rama Rao *et al*. (2016) through conducting monotonic and cyclic load tests on three identical shear wall specimens of medium aspect ratio. An RC shear wall of dimensions 3-m high, 1.56-m wide, and 0.2-m thick loaded axially was tested with pushover loads and cyclic loads. Results revealed that the ratio between the global ductility and local ductility (curvature ductility) is a vital performance feature that controls the post-yield performance of any structure. In the case of squat shear walls and for those walls of medium aspect ratios where l_p is comparable to l such that l_p/l ranges from 0.2 to 0.3, μ_ϕ/μ_Δ (curvature ductility/displacement ductility) varies from 1.2 to 1.7.

3.1.1 Analytical studies

Paulay (1986) presented design procedures for earthquake resistance of ductile reinforced concrete walls. He indicated that the plastic hinge length is primarily a function of the wall length. Based on this, he suggested that the length of plastic hinge area is between $0.5l_w$ and l_w.

Wallace and Moehle (1992) presented an analytical procedure to determine the need of confined boundaries in concrete walls subjected to earthquake loading. They stated that the plastic hinge length is usually between $0.5l_w$ and l_w.

Sasani and Der Kiureghian (2001) developed probabilistic displacement capacity and demand models for RC walls. They derived a model for the plastic hinge length in concrete walls, using the test results reported by Corley (1966) and Mattock (1967). The authors explored several different models, and finally arrived to the following expression

$$\frac{L_p}{d} = \alpha_1 + \alpha_2 \frac{\sqrt{L_s}\, l_s^{3/2}}{d^2} + \xi_L \tag{7}$$

where

l_s is a parameter to make the parameters dimensionless.

ξ_L is model error term.

d is effective depth.

The mean values of α_1 and α_2 were 0.427 and 0.077. The obtained results showed that the above equation provides a better fit to the data, especially for large values of the effective depth which are representative of concrete walls.

For defining numerical models which estimate the deformations and corresponding strength associated with each mechanism, Salonikios (2007) used the results of 11 wall samples with the aspect ratios 1.0 and 1.5. The outcomes revealed that the shear walls with a low aspect ratio experience sliding shear deformations at the plastic hinge area of basement. This failure mode was observed even in the case where the flexural behaviour firstly dominated the structural response. Ignoring such shear deformations leads to miscalculating shear forces at the base of other vertical components. In this regard, in the case of plastic hinge length, the equation proposed by Paulay and Priestley (1992) was used. The calculated displacement ductility showed significant divergence from the experimentally measured ones.

Relying on the results of nonlinear finite element analyses, Bohl and Adebar (2011) proposed an expression for plastic hinge length of RC shear walls as a function of wall length, moment-shear ratio, and axial compression. They selected VecTor2 program for nonlinear finite element analysis as it uses nearly all material models for cracked RC members subjected to shear combined with axial load and bending moment. A procedure to account for the influence of applied shear stress on l_p was also presented. According to the results of 22 analysed isolated walls, the following expression which gives a lower-bound estimate of plastic hinge length was proposed

$$l_p = (0.2l_w + 0.05z)(1 - 1.5P / f_c' A_g) \le 0.8l_w \tag{8}$$

Where l_w= wall length, z = M/V bending moment-to-shear force ratio and P compressive axial load which is taken as positive. The results showed that longer walls (with a larger l_w) have larger shear deformations, and hence, smaller walls have correspondingly larger flexural displacements. Longer walls are generally subjected to larger shear stresses due to the relative flexural stiffness and flexural capacity being larger than the relative shear stiffness.

Smyrou *et al*. (2013) carried out extensive moment-curvature analyses on the T-shaped shear walls. Owing to asymmetric geometry of T-shaped walls, curvature relationships were developed for the yield, serviceability and damage-control limit states. The proposed relationships were presented as a function of compressive axial load ratio and reinforcement ratio for different levels of steel arrangement. The proposed equations were strength independent and allowed the reliable determination of limit-state curvatures which is required in performance-based seismic design method.

Belletti *et al*. (2013) investigated the seismic performance of a common multi-storey RC structural wall building. For evaluating the applicability of some design procedures accepted in buildings having non-rectangular structural walls, several modelling methods were applied for pushover analyses. The results showed that the lumped plasticity model, which is used in current design practice, provided reliable results.

Utilizing the results of nonlinear finite element analyses of cantilever shear walls, Kazaz (2013) proposed a new equation for determining the length of plastic hinge area. For that purpose, by conducting a parametric study, the changes of plastic hinge zone at the basement of cantilever shear wall models was calculated. According to the parametric investigation, the bellow equation was proposed for plastic hinge length of rectangular RC walls

$$L_p = 0.27 L_w \left(1 - \frac{P}{A_w f_c'}\right)\left(1 - \frac{f_y \rho_{sh}}{f_c'}\right)\left(\frac{M/V}{L_w}\right)^{0.45} \tag{9}$$

The parameters were axial load ratio, length of wall, wall horizontal web reinforcement ratio and shear-span-to-wall length-ratio. Accuracy of proposed plastic hinge length equation was verified by using the available shear wall test results. The comparison of results revealed that the length of plastic hinge zone computed from the tensile strain profile is nearly 20% larger than the one calculated using curvature profile.

A parametric study was conducted by Mun and Yang (2015) on the curvature distribution of RC shear wall using a non-linear finite-element analysis procedure. According to the results, a simple model that can reasonably determine the potential plastic hinge region of the shear walls was proposed as below

$$l_p = h_w \left(1 - \frac{M_y}{M_n} + \frac{\Delta M_{shear}}{M_n}\right) \tag{10}$$

Where h_w is wall height, M_n is ultimate moment capacity, M_y is yielding moment and ΔM_{shear} is additional moment owing to diagonal shear crack. The above equation indicates that plastic hinge length decreases in proportion to the ratio of yielding and ultimate moment capacities of shear walls. Whereas, it increases with the increase in the ratio of additional moment owing to the diagonal shear crack and ultimate moment capacity.

An analytical research reported by Bazargani and Adebar (2015) confirmed that large shear strains occur in flexural tension regions of concrete walls due to vertical tension strains in the presence of diagonal cracks and in the absence of demand on the horizontal shear reinforcement. Kara *et al. (*2017) stated that the inter-story drift ratio due to shear strains in the plastic hinge region of a shear wall are equal to approximately 60% of the global drift ratio demand on the wall.

Several equations, which were suggested for predicting the length of plastic hinge area in RC shear walls, were discussed concisely in the preceding section. According to the literature survey, up until now, the plastic hinge length of flanged RC shear walls has been less studied. In addition, an evaluation of the earlier suggested l_p relationships shows that the numerical value of l_p is changeful for the various values of wall length. Hence, an assessment into the length of plastic hinge area of reinforced concrete flanged shear walls is required to reach a consensus about past studies as well as acquire a relationship which can be used to predict l_p more precisely for this type of shear walls.

4. Methodology

4.1 Characteristics of selected ground motions

Structural investigation on the seismic performance of RC flanged shear walls requires the use of recorded ground motions. Because of the correlation between the seismic energy dissipation attributes of the RC structures and the dynamic features of recorded ground motions, the results suitability of nonlinear dynamic analyses depends on the wealth of the selected ground motion data.

When a seismic activity occurs, the amplitude and frequency content of the motion depend on some key parameters such as source characteristics (Stewart *et al.* 2002) and the characteristics of the soil or rock layers between the site free field and the focus (NEHRP 2011). Due to these sources, each selected ground motion displays different characteristics in terms of time duration, amplitude and frequency content. According to the past studies, in this paper, the frequency content of ground motion has been considered to be the most important factor interfering in the nonlinear response of reinforced concrete structures. Relying on the review of earlier studies and examining the earthquake records, Pavel and Lungu (2013) revealed three groups of earthquake ground motions including (a) 'normal' ground motions with rich energy content over a wide-ranging frequencies which display an irregular acceleration form (0.8 g/m/s ≤ PGA/PGV ≤ 1.2 g/m/s); (b) ground motions demonstrating big amplitude and high frequency vibrations in the strong motion part of the motion (PGA/PGV > 1.2 g/m/s; (c) ground motions comprising limited intense and long duration acceleration pulses (PGA/PGV < 0.8 g/m/s).

As a result, a total of 7 ground motion records were opted to consider a wide range of frequency content. Hence the selected ground motions were acquired within 15 km of the contributing fault plane in the magnitude (M_W) domain of 6.5 to 7.4 based on the Richter scale.

Additional information about the selected earthquake

Table 1

	Earthquake	Year	Station	Component	Magnitude (M_w)	Distance	PGA (g)	PGV (cm/s)	PGD (cm)	PGA/PGV (g/m/s)
1	Tabas	1978	Tabas	TR	7.4	3	0.85	121.4	95.06	0.7
2	Loma Prieta	1989	LGPC	00	7.0	1.3	0.56	94.71	41.13	0.59
3	Cape Mendocino	1992	Petrolia	90	7.1	9.5	0.66	89.68	28.99	0.73
4	Kocali	1999	Duzce	DZC180	7.4	12.7	0.312	58.8	44.11	0.53
5	Imperial Valley	1979	ELCentro Array #2	H-E02140	6.5	16.1	0.42	31.5	14.34	1.35
6	Northridge	1994	Sylmar	360	6.7	6.4	0.84	129.3	31.92	0.65
7	Bam	2003	Bam	L1	6.5	7	1.09	111.26	89.24	0.98

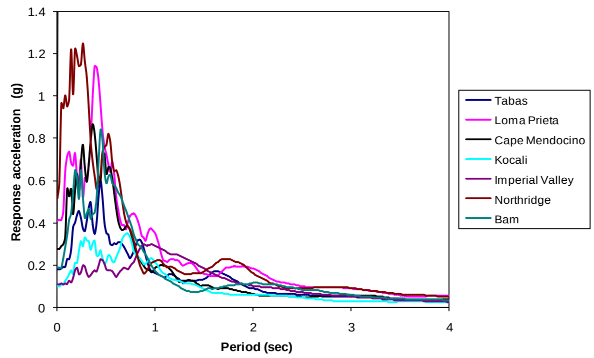

Fig. 4 Acceleration response spectra of selected ground motions

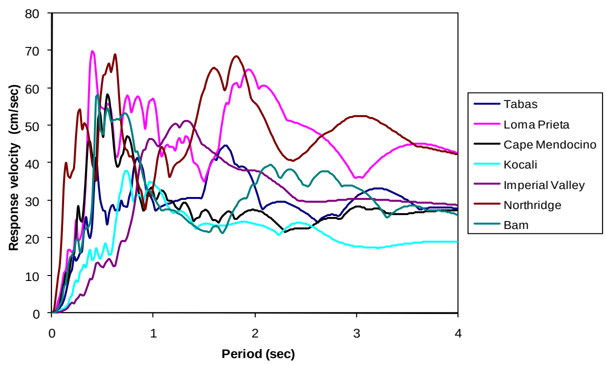

Fig. 5 Velocity response spectra of selected ground motions

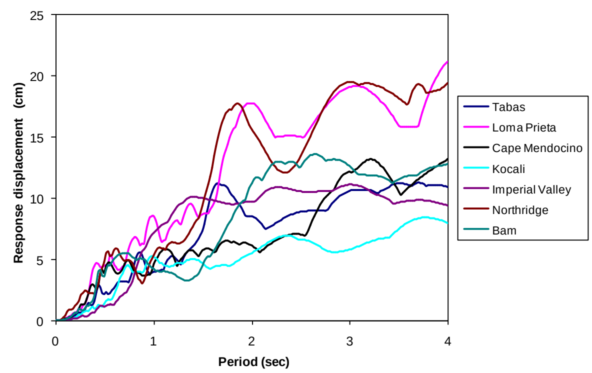

Fig. 6 Displacement response spectra of selected ground motions

ground motions including year, recording station, utilized component of the record, and maximum earthquake properties comprising peak ground acceleration (PGA), velocity (PGV), and displacement (PGD) have been tabulated in Table 1.

The response spectra of displacement, velocity and acceleration of selected ground motions have been shown in Figs. 4 to 6 respectively. Employed in this research work is a spectral matching procedure proposed by Somerville (2005). PGA/PGV ratio, Drms technique and scale factors applied to match the spectra were the criteria to select the most suitable ground motions.

4.2 Verification of analytical models

The efficiency and precision of the used finite element program and analytical models in determining the nonlinear response of RC flanged shear walls is confirmed by comparing the numerical and corresponding experimental measurements. For this purpose, experimentally tested shear wall specimens of Palermo and Vecchio (2002) and some other experimental research works (Combescure and Sollogoub 2011, Thomsen and Wallace 2004, Mehmood *et al.* 2015, Brueggen *et al.* 2017) were selected with various aspect ratios, reinforcing steel layouts and loading conditions. Full details of verifications have been reported by Ghaderi Bafti (2018). For brevity, the comparison of analytical modelling with the experimental work of Palermo and Vecchio (2002), which was conducted in the University of Toronto, is presented here.

4.2.1 Material modeling

Because of progressive cracking at the contact between mortar and aggregates (transition zone), concrete has different behavior under the various combinations of loads. Increasing and propagating these cracks under the loading cause nonlinear behavior of the concrete. As shown in Fig. 7, the stress-strain curve of concrete used in this research work comprises two sections. The rising branch up to the peak compressive strength is represented by the equation proposed by Ashour and Morley (1993)

$$\sigma = \frac{E_0 \, \varepsilon}{1 + \left(\frac{E_0}{E_{sc}} - 2\right)\left(\frac{\varepsilon}{\varepsilon_{max}}\right) + \left(\frac{\varepsilon}{\varepsilon_{max}}\right)^2} \qquad (11)$$

where E_0 is the initial modulus of elasticity of the concrete, E_{sc} is the secant modulus of the concrete at the peak stress, σ is stress, ε is strain and ε_{max} is the strain at peak stress. The downward, or the strain-softening, branch is idealized by the Bazant *et al.* (1986) model

$$\sigma = \sigma_c \left(\frac{\varepsilon}{\varepsilon_{max}}\right) \exp\left(1 - \varepsilon/\varepsilon_{max}\right) \qquad (12)$$

where σ_c is compressive strength of the concrete. For uniaxially loaded concrete, σ_c is equal to f_c. The concrete is considered crushed once the equivalent compressive strain in the major directions exceeds the ultimate compressive strain of the concrete, ε_{cu}. For removing numerical difficulties after crushing ($\varepsilon > \varepsilon_{cu}$) and cracking of the concrete ($\varepsilon > \varepsilon_{tu}$), a small value is allocated to the concrete compressive and tensile stresses, $\gamma_c f_c$ and $\gamma_t f_t$ (Fig. 9), where parameters γ_c and γ_t describe the residual compressive and tensile strength factors, respectively.

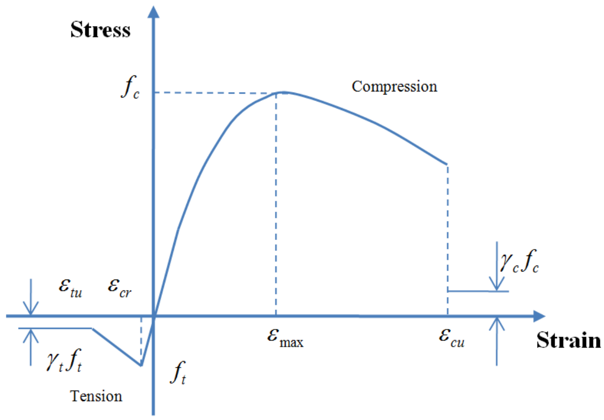

Fig. 7 The stress-strain relationship of concrete

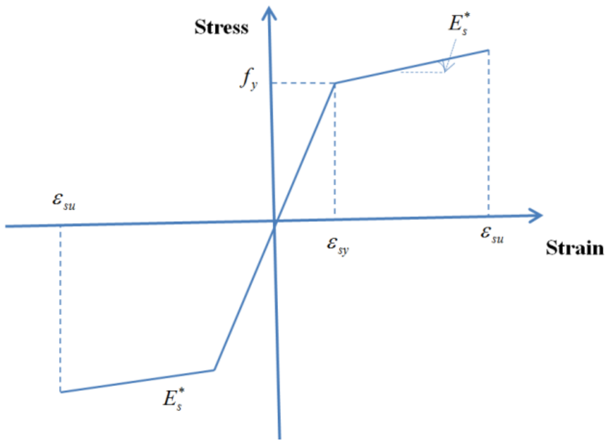

Fig. 8 The stress-strain relationship of steel

Numerous parameters affect the cracking behavior of concrete structures. Concrete tensile cracking is an important nonlinear factor in the concrete structural components. Concrete cracking not only reduces stiffness, but also makes it possible to redistribute moment as well as increase the bond stress at the steel-concrete interface. Concrete cracking is simulated using the fixed smeared cracking model. In this model, the crack occurs when the main tensile stress goes beyond the limit of concrete tensile strength. After cracking, elastic modulus perpendicular to the crack direction is decreased to a very small value.

The steel reinforcing bars are simulated as an elastic strain-hardening material as shown in Fig. 8. The steel bars can be presented either as smeared layers or as individual bars.

4.2.2 Geometric modeling

Palermo and Vecchio (2002) examined the response of two full scale flanged shear wall structure under the cyclic loading. The specimens were a single story flanged shear wall with h_w/l_w= 0.67. The tested samples were built with nearly rigid slabs on top and bottom. The top slab

Table 2 Properties of concrete material

Zone	f'_c (MPa)		ε_c (MPa($\times10^{-3}$))	
	DP1	DP2	DP1	DP2
Wall Web	21.7	18.8	2.04	2.12
Wall Flange	21.7	18.8	2.04	2.12
Top Slab	43.9	38.0	1.93	1.96
Bottom Slab	34.7	34.7	1.66	1.66

Table 3 Properties of steel material

Zone	Type	Diameter (mm)	ε_{sy} ($\times10^{-3}$)	f_{sy} MPa	f_{su} MPa
Wall Web	D6	7	3.18	605	652
Wall Flange	D6	7	3.18	605	652
Top Slab	No. 30	29.9	2.51	550	696
Bottom Slab	No. 30	29.9	2.51	550	696

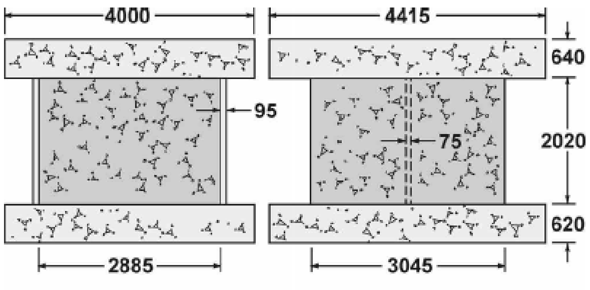

(a) (b)

Fig. 9 Test specimen details: (a) side view; (b) end view

(2600×1440×150 mm) was used to distribute the axial and cyclic lateral load to the shear wall. The bottom slab (2600×1440×300 mm) was attached to the rigid floor of the lab to act as a rigid foundation.

Reinforcement bars of D6, which were spaced 140 mm horizontally and 130 mm vertically in two parallel layers, were utilized to reinforce wall web. The 95 mm shear wall flanges were also reinforced with this arrangement near the wall web, but near the tips of flanges the distance increase to 255 mm. Dimensions and sizes of the shear walls and reinforcing arrangement have been shown in Figs. 9 and 10, respectively. Characteristics of concrete and steel materials have been tabulated in Tables 2 and 3.

The RC flanged shear wall shown in Figs. 8 and 9 were modeled as indicated in Fig. 11, which shows classic finite element (FE) meshing selected for discretization of the shear walls. The mesh size used in FE analysis must be adequately fine to obtain the concrete behaviour precisely. The load-carrying capacity of a structural-concrete member is said to be "size-effect" dependent when its predicted values depend on the size of the member. The dependency of results on the finite element size arises basically from the use of the smeared, or the discrete cracking models based on the strength concept.

Researchers point out that the numerical analysis results of concrete structures are greatly dependent on the finite element mesh size used in modeling and are therefore affected by the tension stiffening effect in the concrete (Mortezaei and Kheyroddin 2009). Hence, in addition to the original model, five extra models with the mesh size of 50, 100, 150, 200, 250 and 300 mm were created to check the mesh size dependency of the results. The results (Table 4)

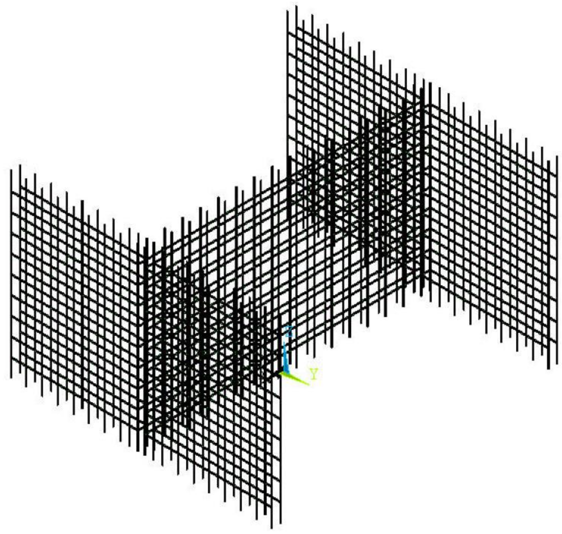

Fig. 10 Top view of wall reinforcement

Table 4 The cracking, yielding and ultimate loads of the selected flanged shear wall for different meshes

Number of Elements	Size of Element (mm × mm)	Cracking Load (kN)	Yielding Load (kN)	Ultimate Load (kN)	P_u (Anl.) / P_u (Exp.)
7047	50 × 50	509	1933	5449	1.046
6210	100 × 100	510	1930	5372	1.031
5406	150 × 150	510	1922	5190	0.996
4624	200 × 200	510	1905	5137	0.986
3843	250 × 250	512	1887	5086	0.976
3019	300 × 300	512	1871	4923	0.945
Experimental result	---	511	1912	5210	---

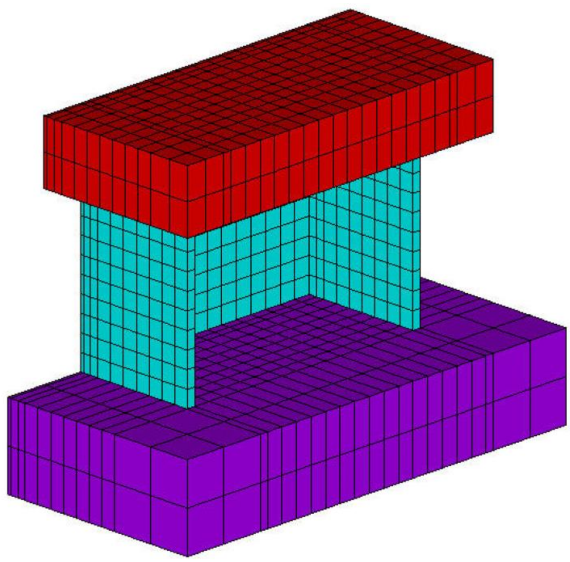

Fig. 11 Finite element mesh configuration

Table 5 Comparing the numerical and corresponding experimental measurements

Type of Analysis	Cracking Load (kN)	Yielding Load (kN)	Ultimate Load (kN)	P_u (Anl.) / P_u (Exp.)
FE analysis	510	1922	5190	0.996
Experimental result	511	1912	5210	---

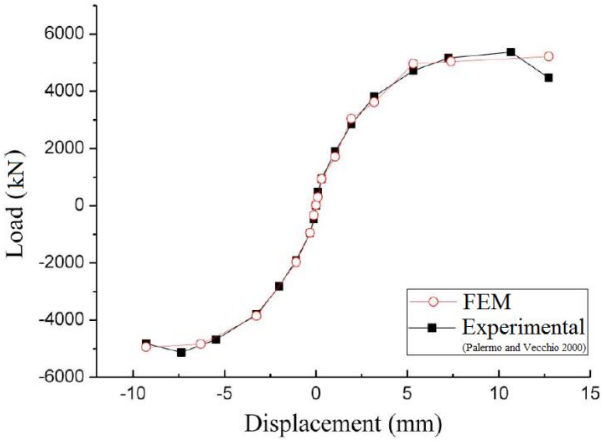

Fig. 12 Load-displacement relationship at the top of shear wall

showed that there is a considerable difference between the results of the fine and coarse mesh models. According to the results, the appropriate mesh size, i.e., 150×150, was selected for further analysis purposes.

Also, on the top, bottom and side faces of the shear wall models, the web steel reinforcing was uniformly distributed along the boundaries of the brick elements in the longitudinal and transverse directions.

The FE meshing presented in Fig. 11 consisted of 5406 solid elements and corresponding 31171 nodes. Because of similarity, half of the test specimen was modeled. The meshing area was separated into four zones: web, flanges, top slab, and bottom slab. For modeling I-shaped shear wall specimen, 27-node Lagrangian brick elements have been used for concrete modeling, while the reinforcing bars were simulated using 3-node parabolic elements with axial stiffness. The adopted embedded parabolic elements connect the intersections of the rebar axes with the faces of the 3D-solid concrete elements.

4.2.3 Verification results

Backbone curve of cyclic loading of analytical model is compared with the measured values, as shown in Fig. 12. Comparing the numerical and corresponding experimental measurements (Table 5) shows that the FE program prepares rational results and as such could be used to estimate the nonlinear behavior of RC shear walls under the dynamic loading. At the last step of loading the inclination angle of the principal compressive strains was approximately 45 degrees. Under the increasing shear forces, both the principal compressive and tensile strains increased equivalently. The plastic strain and cracking pattern in the wall web were matched well with the experimental results.

Table 6 Estimated length of plastic hinge area under the various levels of axial load (in m)

Axial Load	Tabas	Loma Prieta	Cape Mendocino	Kocaeli	Imperial Valley	North ridge	Bam	Average
0	1.7	1.682	1.769	1.74	1.856	1.769	1.769	1.76
0.1	1.74	1.711	1.798	1.769	1.827	1.682	1.769	1.76
0.2	1.755	1.701	1.674	1.647	1.782	1.566	1.809	1.70
0.3	2.125	2.106	2.08	2.236	2.184	2.158	2.236	2.16
0.4	2.3	2.2995	2.0805	2.409	1.971	2.0367	2.1462	2.18
0.5	2.4	2.295	2.04	2.21	2.21	1.87	2.193	2.17
0.6	2.5	2.38	2.295	2.55	2.465	2.21	2.431	2.40
0.7	2.64	2.635	2.669	2.805	2.805	2.55	2.737	2.69
0.8	2.8	2.848	2.88	2.88	2.848	2.72	2.784	2.82

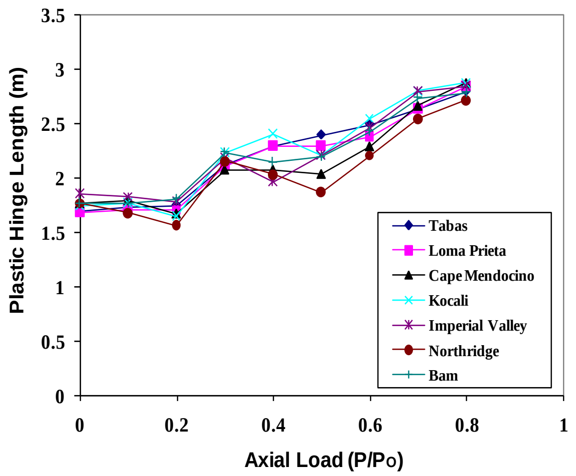

Fig. 13 The length of plastic hinge area and axial load levels relationship

To sum up, in this section, with the finite element modelling of the flanged RC shear wall tested by Palermo and Vecchio and comparing the results such as cracking, yielding and ultimate limit loads as well as cracking pattern, it was found that the deviation of the analytical results is very low compared to the experimental ones and is less than 1%. Taking into account many unknown input variables, however, this level of precision is considered as acceptable.

5. Parametric study

Relying on the literature review, many parameters are involved in the length of plastic hinge area. Some of the main factors, which affect the response of structural walls, are as follows: 1) the ratio of walls cross-sections to floor-plan area, 2) fundamental period, 3) shape of wall cross-section, 4) wall aspect ratio and configuration in the plan, 5) wall axial load, 6) arrangement and percentage of longitudinal reinforcing, 7) degree of confinement of compression zone concrete, 8) behavior modes of the wall, 9) different characteristics of earthquakes and so on.

Here and in this level, numerous nonlinear time-history analyses have been carried outed to determine the

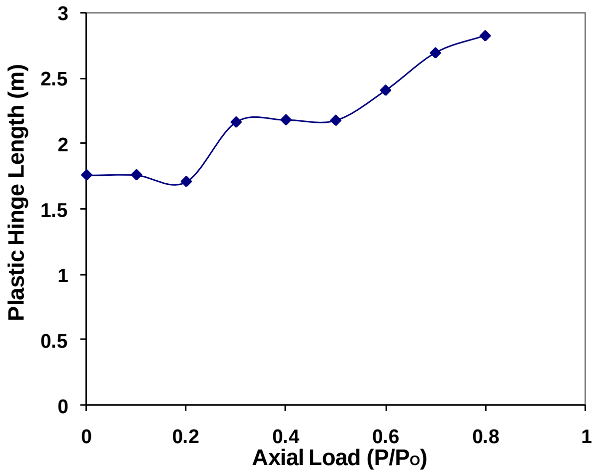

Fig. 14 Comparing the relation between the levels of axial load and the length of plastic hinge area

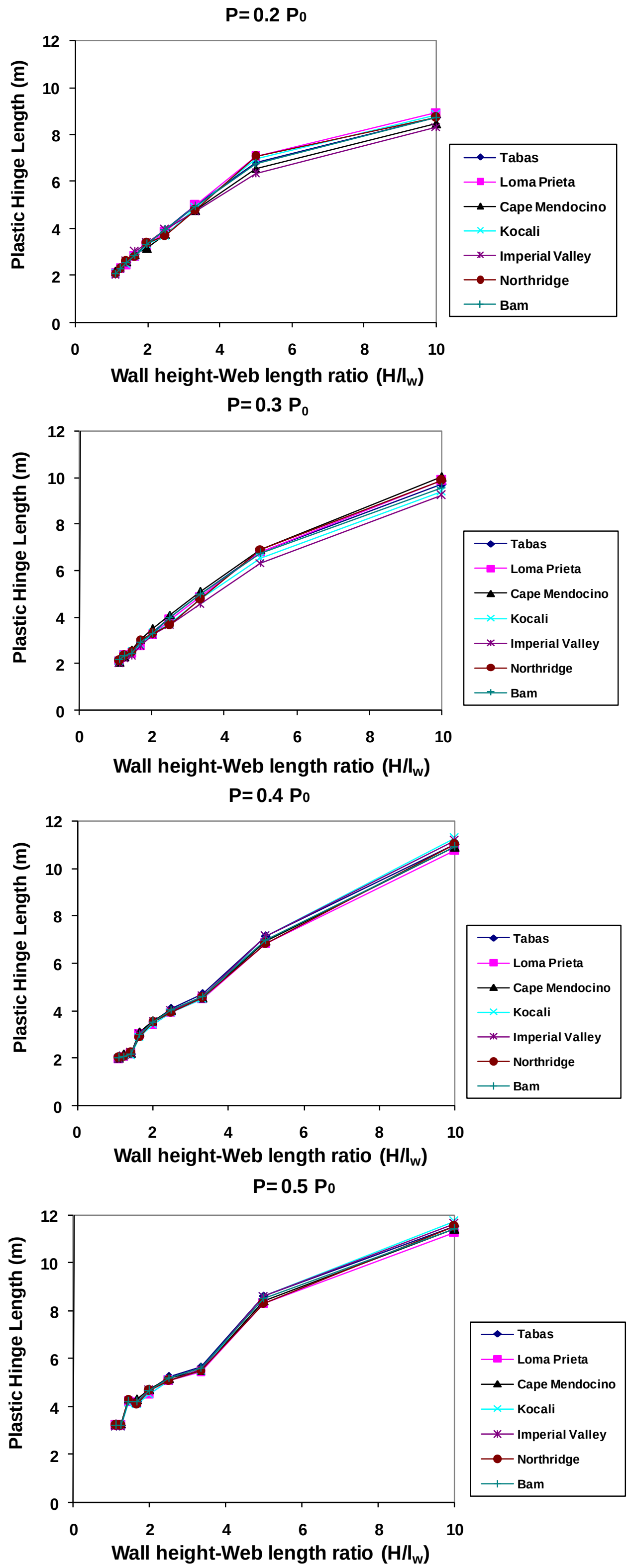

Fig. 15 Relationship between the length of plastic hinge area and height-web length ratio for different levels of axial load

characteristics of plastic hinge region in the RC flanged shear walls. This is done by applying a finite element program, and obtained results are compared with the equivalent experimental records. The FE program is able to calculate large deformation behavior of structural components, taking into consideration geometric nonlinearities as well as material inelasticity. The used approach represents developing material nonlinearity alongside the length and cross-sectional region of the component. By means of this approach, the length of yield area and accurate amount of inelastic rotation can be defined devoid of utilizing the concept of equivalent plastic hinge length. As presented in previous sections, Fig. 3 demonstrates how to compute the analytical inelastic rotation and equivalent length of plastic hinge area. The summary of this procedure is as follows. After determining the ultimate limit curvature alongside the member based on the concrete and steel strains in the compression and tension zone, respectively, the plastic rotation is achieved by integrating along the length of yield zone. This length is an area between the points of ultimate and yield curvatures. Then, the equivalent length of plastic hinge zone is determined based on the inelastic rotation.

Relying on the sensitivity analysis and utilizing the above technique, the effect of different variables such as axial load level (P/P_o), height-web length ratio (H/l_w), and wall web-flange length ratio (l_w/l_f), on l_p under the effect of various ground motions are studied. In the nonlinear analysis, the modulus of elasticity (Young's modulus) E = 30 kN/mm^2, Poisson's ratio $\nu = 0.20$ and the mass density ρ = 24 kN/m^3 are assumed in all models. The steel reinforcing bars are modelled with yield and ultimate strengths of 400 MPa and 600 MPa, respectively.

5.1 Axial load level

The important effect of variations in the axial force demand of the shear walls can be attributed to the fluctuation in the shear capacity of the walls. Dependence of shear capacity of the structural walls on the axial force is a well-known subject in the seismic design of RC structures. That means enhancing the axial force demand in the shear wall can leads to an increase in the shear capacity of the structural wall which is helpful for the seismic performance of the shear wall.

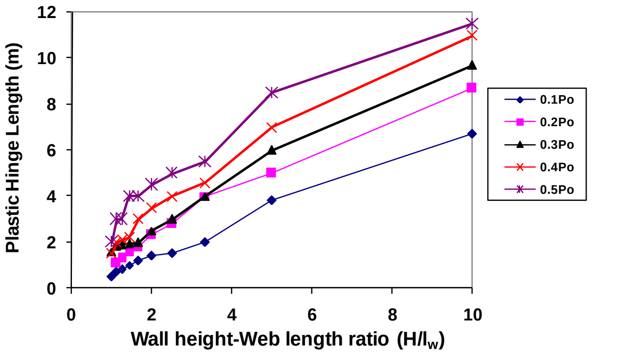

Fig. 16 Relationship between the length of plastic hinge area (average) and height-web length ratio for different levels of axial load

In this regard, to evaluate the influence of axial load on the characteristics of plastic hinge area subjected to the earthquake loading with different frequency content, 180 inelastic dynamic analyses were carried out. The reinforced concrete flanged shear walls with different intensities of axial load under the 7 selected records were studied. The other parameters such as wall web and flange length as well as wall height were kept constant respectively. Table 6 and Fig. 13 demonstrate the obtained results of the dynamic analyses. For the entire models assessed in Fig. 14, the length of the plastic hinge area is determined utilizing the route explained formerly.

The results show that the presence of axial load on a wall that is loaded seismically results in an increase in its flexural capacity and shear strength which cause an increase in plastic hinge length. On the whole, axial compression reduces shear distortion and increases the shear stiffness of the hinging region.

The results show that for flanged RC shear walls, the length of the area where high inelastic curvatures expand will be larger than the corresponding plastic hinge area recommended by many codes. For that reason, the necessary length for close spacing transverse reinforcing requires to be larger than the predicted length of the plastic hinge area by many codes. In summary, the potential l_p identified by the codes is not acceptable for flanged shear walls sustaining high levels of axial load.

5.2 Ratio of height to web length (H/l_w)

With the aim of examining the effect of H/l_w on the characteristics of plastic hinge area, 420 inelastic seismic analyses were carried out. The flange shear walls with a variety range of axial loads and height on web length ratios under the 7 selected earthquake records were evaluated. For this phase of parametric study, the flange length was fixed to a invariant value. The obtained results of dynamic analyses are presented in Figs. 15 and 16.

As can be observed in Fig. 15, for a constant level of axial load, l_p increases as increasing H/l_w. For low levels of axial load (≈ 0.2Po), the enhancement observed in l_p with enhancing H/l_w is lower than high levels of axial load. For a specified H/l_w, the l_p increases with the increasing the levels of axial load. The enhancements in l_p detected at low levels

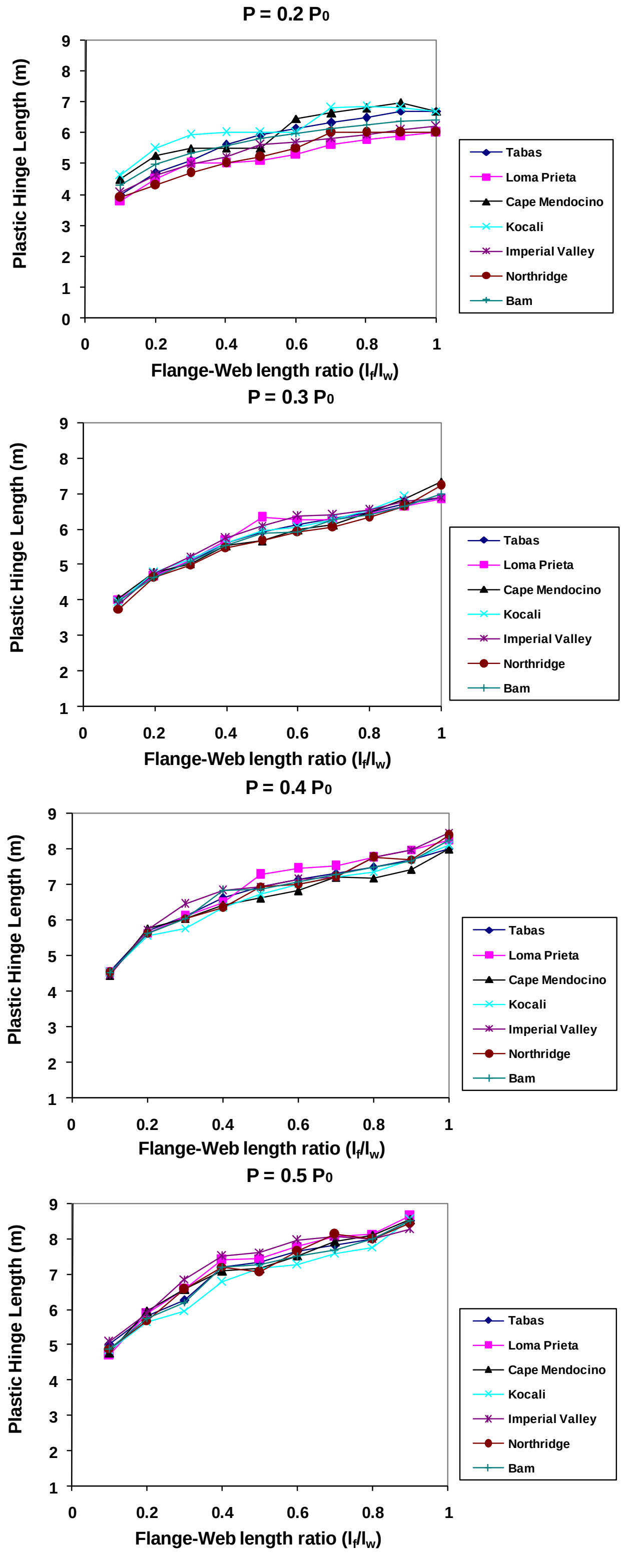

Fig. 17 The relation between the length of plastic hinge area and flange to web length ratio for a range of axial load levels

of H/l_w are less distinguished than those examined at higher H/l_w values. Comparing between outcomes in this study and past studies shows that the length of plastic hinge area in RC flanged shear walls is higher than the plastic hinge length of RC rectangular shear walls.

The comparison between different levels of plastic hinge length shows when the number of stories increase, influence of shear wall length rather than increased axial load become more prominent in enhancing the rigidity of structural system. The influence of enlarged wall height for managing the length of plastic hinge area is also visible in Fig. 16. It is justified such that flanged shear walls with larger length offer much better control and decrease on the drift ratio demands. For decreasing the lateral drift ratio demands under the seismic loading, the more effective parameter is wall stiffness supplied by the enhanced moment of inertia in comparison with the wall cross sectional area.

5.3 Flange to web length ratio (l_f/l_w)

Past earthquakes experiences and analytical results demonstrate that structural shear walls with flanges behave more effective than walls without flanges. Fundamentally, the presence of wall flanges and continuously varying axial load in the walls combine to create a structure with distinctly different strength and stiffness characteristics in the two loading directions.

Hence, in this section, with the purpose of evaluating the influence of l_f/l_w on the plastic hinge length, 420 inelastic time-history analyses were carried out. The flange shear walls with a variety of axial load levels and flange over web length ratios under the 7 selected seismic records were examined. This phase of parametric study was done with a constant value of web length. The results of nonlinear analyses have been presented in Figs. 17 and 18.

From the results, considering the wall aspect ratio and axial load, it is deduced that structural shear walls with flanges can stand higher levels of seismic lateral load than structural walls without flanges. Accordingly, for bearing lateral loads generated by earthquake ground motions the effect of flanges must be regarded when determining the capacity and ductility of shear walls. The results also show that for the ground motions which have lower PGA/PGV ratio the plastic hinge length is higher than those for normal and high PGA/PGV ratio.

5.4 Suggested relationship for the length of plastic hinge area

Numerous parameters may be affect the length of plastic hinge area, which of them can be mentioned as follows: 1) the shape of structural wall; 2) the strength of materials constituting structural wall such as concrete and steel; 3) arrangement layout of longitudinal reinforcing steel; 4) intensity of axial load; 5) distribution and fluctuation of bending moment; 6) the amount of shear demand in the plastic hinge zone; 7) the volume and mechanical properties of transverse reinforcing steel; 8) amount and geometry of confinement in the possible plastic hinge region; and 9) various characteristics of seismic ground motions. Past recommended simple relationship which presented in the literature review do not include the entire or even the majority of the abovementioned parameters. That’s why large discrepancy exists in the length values of plastic hinge area determined utilizing these tentative relationships, as demonstrated clearly in previous. Thomsen and Wallace (2004), in their work, considered most of the parameters affecting the length of plastic hinge region. They found that the contribution of the longitudinal reinforcement effect is not considerable.

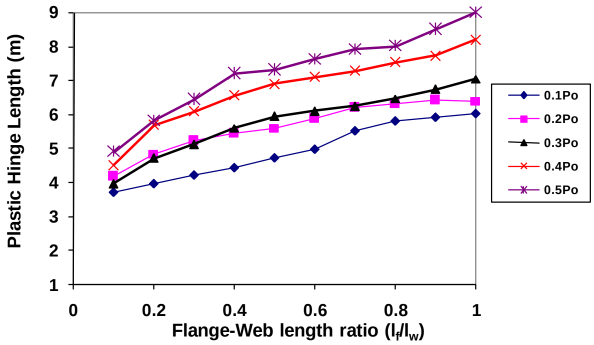

Fig. 18 The relation between the length of plastic hinge area (average) and flange to web length ratio for a range of axial load levels

Table 7 Estimated plastic hinge length by various expressions

Selected Source	Mattock	Paulay	Bohl & Adebar	Kazaz	Mun & yang	Measured	Proposed equation
NEES: shear wall database	$0.57l_w$	$0.49l_w$	$0.70l_w$	$0.88l_w$	$0.80l_w$	$1.02l_w$	$1.07l_w$
UCLA-RC walls database	$0.62l_w$	$0.52l_w$	$0.80l_w$	$0.91l_w$	$0.96l_w$	$1.15l_w$	$1.18l_w$
Thomsen and Wallace	$0.60l_w$	$0.49l_w$	$0.70l_w$	$0.43l_w$	$0.72l_w$	$0.61l_w$	$0.63l_w$
Palermo and Vecchio	$0.52l_w$	$0.49l_w$	$0.70l_w$	$0.49l_w$	$0.72l_w$	$0.59l_w$	$0.63l_w$

Based on the numerical outcomes found in this research work, the subsequent equation is suggested for predicting the length of plastic hinge area in the RC flanged shear walls

$$l_p = \left[1 + 0.35\left(\frac{P}{P_0}\right) + 0.15\left(\frac{H}{l_w}\right) + 0.55\left(\frac{l_f}{l_w}\right)\right] \times 0.22\ l_w \qquad (13)$$

In this equation, H is shear wall height, P is the applied level of axial load, P_0 is the nominal capacity of axial load, l_w is the wall web length and l_f is the wall flange length. This relationship evaluate satisfactorily with the examined values in this paper and measured amounts reported in the Thomsen and Wallace (2004) and Palermo and Vecchio experimental work (Palermo and Vecchio 2002).

To explore the precision of above equation, the length of plastic hinge area in the flanged RC shear wall samples which were studied by Thomsen and Wallace (2004) and Palermo and Vecchio experimental work (Palermo and Vecchio 2002), were predicted utilizing a variety of equations and contrasted with the measured length of plastic hinge area (Table 7).

The consequence of assessment showed that using the suggested relationship, rational predictions can be obtained for the length of plastic hinge area in the RC flanged shear walls under the various levels of axial load and seismic loading. Moreover, the assessment result of suggested relationship and some earlier expressions show that utilizing some relationships can miscalculate the length of plastic hinge area in the RC shear walls. However, the suggested expression can determine reasonably the length of plastic hinge region in the RC flanged shear walls under the variety levels of axial loads.

6. Conclusions

Structural modeling in the nonlinear range contains high complications, particularly for the great number of parameters that must be accounted for. The problem is more difficult for reinforced concrete structures, due to the computational problems arising in the reproduction of the nonlinear behavior of constituent materials. In this regard, this research work developed the outcome of an extensive analytical evaluation regarding the length of plastic hinge area in the flanged RC shear walls. Numerous inelastic time history analyses have been carried out with the aim of examining the characteristics of plastic hinge regions, and the results have been presented. Some of the key concluding remarks achieved based on the results are as follows:

1. The analytical outcomes demonstrate good relevancy with the existing experimental data and confirm the advantageous of inelastic finite element analysis as an influential and potent tool to evaluate the performance of various forms of RC components under the earthquake loading.

2. The behavior of flanged shear walls is considerably different from that of rectangular structural walls in the viewpoint of cracking pattern, seismic performance, stiffness, ductility and ultimate strength.

3. Flanged shear walls have high flexural strength as compared to rectangular shear walls. This is because limited vertical reinforcement which be placed near the edges of the rectangular wall. As a result, for the same height, the level of shear stress in the web of rectangular walls is usually less than that in flanged sections.

4. Because of the flanges, flanged shear walls are less prone to lateral instability of the compressive region; and have large in-plane and out-of-plane stiffness and develop high shear stresses. Greater resistance is provided against sliding shear due to the flanges.

5. For the ground motions which have lower PGA/PGV ratio the plastic hinge length is higher than those for normal and high PGA/PGV ratio.

6. The results demonstrate that the possible length of plastic hinge area defined by many codes is not acceptable for flanged shear walls and may even be non-conservative in some statuses. Hereupon, the length of the area in which close spacing transverse reinforcing steel are employed is recommended to increase from $1.0l_w$ to $2.0l_w$.

7. The main benefit of flanges is that it leads to modest increases in both the in-plane load and displacement capacities of the element, because it increases the moment arm between the resultant tensile and compressive forces in the wall element.

8. The suggested equation in this paper, offer more vision for realizing the characteristics of plastic hinge area in the RC flanged shear walls and result in a more accurate prediction of the plastic hinge length in these components subjected to a variety of frequency content of ground motions.

References

ACI Committee 318 (2014), *Building Code Requirements for Structural Concrete:(ACI 318-14), and Commentary (ACI 318R-14)*, American Concrete Institute, Farmington Hills, Michigan, U.S.A.

ASCE/SEI 7-16 (2017), *Minimum Design Loads and Associated Criteria for Buildings and Other Structures*, American Society of Civil Engineers, Reston, Virginia, U.S.A.

ASCE/SEI 41-17 (2017), *Seismic Evaluation and Retrofit of Existing Buildings*, American Society of Civil Engineers, Reston, Virginia, U.S.A.

Ashour, A.F. and Morley, C.T. (1993), "Three-dimensional nonlinear finite element modelling of reinforced concrete structures", *Fin. Elem. Analy. Des.*, **15**(1), 43-55.

Bazargani, P. and Adebar, P. (2015), "Interstory drifts from shear strains at base of high-rise concrete shear walls", *J. Struct. Eng.*, **141**(12), 04015067.

Belletti, B., Damoni, C. and Gasperi, A. (2013), "Modeling approaches suitable for pushover analyses of RC structural wall buildings", *Eng. Struct.*, **57**, 327-338.

Belytschko, T., Bažant, Z.P., Yul-Woong, H. and Ta-Peng, C. (1986), "Strain-softening materials and finite-element solutions", *Comput. Struct.*, **23**(2), 163-180.

Bohl, A. and Adebar, P. (2011), "Plastic hinge lengths in high-rise concrete shear walls", *ACI Struct. J.*, **108**(2), 148-157.

Brueggen, B.L., French, C.E. and Sritharan, S. (2017), "T-shaped RC structural walls subjected to multidirectional loading: Test results and design recommendations", *J. Struct. Eng.*, **143**(7), 04017040.

Christidis, K., Vougioukas, E. and Trezos, K.G. (2013), "Seismic assessment of existing RC shear walls non-compliant with current code provisions", *Mag. Concrete Res.*, **65**(17), 1059-1072.

Combescure, D. and Sollogoub, P. (2011), *IAEA CRP-NFE CAMUS Benchmark Experimental Results and Specifications to the Participants Annex III*, International Atomic Energy Agency (IAEA), 19-76.

Corley, W.G. (1966), "Rotational capacity of reinforced concrete beams", *J. Struct. Div.*, **92**(ST5), 121-146.

CSA A23.3-14 (2014), *Design of Concrete Structures-A National Standard of Canada*, Canadian Standards Association (CSA).

EN 1992-1-1 (2004), E*urocode 2: Design of Concrete Structures-Part 1-1: General Rules and Rules for Buildings*, European Committee for Standardization, Brussel, Belgium.

Ghaderi Bafti, F. (2018), "Characteristics of plastic hinge area in the flanged reinforced concrete shear walls", Ph.D. Dissertation, Islamic Azad University, Iran.

Kara, I., Ashour, A. and Dundar, C. (2017), "Analysis of R/C frames considering cracking effect and plastic hinge formation", *Struct. Eng. Mech.*, **63**(5), 669-681.

Kazaz, İ. (2013), "Analytical study on plastic hinge length of structural walls", *J. Struct. Eng.*, **139**(11), 1938-1950.

Mattock, A.H. (1967), "Discussion of 'rotational capacity of reinforced concrete beams' by W.G. Corley", *J. Struct. Div.*, **93**(ST2), 519-522.

Mehmood, T., Hussain, K. and Warnitchai, P. (2015), "Seismic evaluation of flexure-shear dominated RC walls in moderate seismic regions", *Mag. Concrete Res.*, **67**(18), 1003-1016.

Mortezaei, A. and Kheyroddin, A. (2009), "Size effects in reinforced concrete flanged shear walls", *Int. J. Civil Eng.*, **7**(1), 27-40.

Mortezaei, A. and Ronagh, H.R. (2012), "Plastic hinge length of reinforced concrete columns subjected to both far-fault and near-fault ground motions having forward directivity", *Struct. Des. Tall Spec. Build.*, **22**(12), 903-926.

Mun, J.H. and Yang, K.H. (2015), "Plastic hinge length of reinforced concrete slender shear walls", *Mag. Concrete Res.*, **67**(8), 414-429.

NEHRP, C.J.V. (2011), *Selecting and Scaling Earthquake Ground Motions for Performing Response-History Analyses*, NIST GCR 11-917-15, 256.

Oesterle, R.G., Aristizabal-Ochoa, J.D., Shiu, K.N. and Corley, W.G. (1984), "Web crushing of reinforced concrete structural walls", *ACI J.*, **81**(3), 231-241.

Palermo, D. and Vecchio, F.J. (2002), "Behavior of three-dimensional reinforced concrete shear walls", *ACI Struct. J.*, **99**(1), 81-89.

Panagiotakos, T.B. and Fardis, M.N. (2001), "Deformations of reinforced concrete members at yielding and ultimate", *ACI Struct. J.*, **98**(2), 135-148.

Paulay, T. (1986), "The design of ductile reinforced concrete structural walls for earthquake resistance", *Earthq. Spectr.*, **2**(4), 783-823.

Paulay, T. and Priestley, M.J.N. (1992), *Seismic Design of Reinforced Concrete and Masonry Buildings*, John Wiley & Sons.

Paulay, T. and Priestley, M.J.N. (1993), "Stability of ductile structural walls", *ACI Struct. J.*, **90**(4), 385-392.

Pavel, F. and Lungu, D. (2013), "Correlations between frequency content indicators of strong ground motions and PGV", *J. Earthq. Eng.*, **17**(4), 543-559.

Preti, M. and Giuriani, E. (2011), "Ductility of a structural wall with spread rebars tested in full scale", *J. Earthq. Eng.*, **15**(8), 1238-1259.

Rao, G.V.R., Gopalakrishnan, N., Jaya, K.P., Muthumani, K., Reddy, G.R. and Parulekar, Y.M. (2016), "Studies on nonlinear behavior of shear walls of medium aspect ratio under monotonic and cyclic loading", *J. Perform. Constr. Facilit.*, **30**(1), 04014201.

Salonikios, T. (2007), "Analytical prediction of the inelastic response of RC walls with low aspect ratio", *J. Struct. Eng.*, **133**(6), 844-854.

Sasani, M. and Kiureghian, A. (2001), "Seismic fragility of RC structural walls: Displacement approach", *J. Struct. Eng.*, **127**(2), 219-228.

Smyrou, E., Sullivan, T., Priestley, N. and Calvi, M. (2013), "Sectional response of T-shaped RC walls", *Bullet. Earthq. Eng.*, **11**(4), 999-1019.

Somerville, P. (2005), *Guidelines for the Selection, Modification and Scaling of Ground Motion Time Histories*, URS, SCEC, COSMOS Annual Meeting, San Francisco, U.S.A.

Stewart, J.P., Chiou, S.J., Bray, J.D., Graves, R.W., Somerville, P.G. and Abrahamson, N.A. (2002), "Ground motion evaluation procedures for performance-based design", *Soil Dyn. Earthq. Eng.*, **22**(9-12), 765-772.

Thomsen, J. and Wallace, J. (2004), "Displacement-based design of slender reinforced concrete structural walls-experimental verification", *J. Struct. Eng.*, **130**(4), 618-630.

Wallace, J. and Moehle, J. (1992), "Ductility and detailing requirements of bearing wall buildings", *J. Struct. Eng.*, **118**(6), 1625-1644.

CC

Notation

A_g	gross area of section
A_s	area of tension reinforcement
c	distance from extreme compression fiber to neutral axis
d	effective depth of cross section
f_c'	compressive strength of concrete
f_{cu}	characteristic compressive strength of concrete
f_y	yield stress of reinforcement
f_{sy}	yield strength of reinforcement
f_{su}	ultimate strength of reinforcement
H	distance from critical section to point of contraflexure
L	wall height
l_f	wall flange length
l_p	plastic hinge length
l_y	yielding length
l_w	wall web length
M_{cr}	bending moment at cracking limit
M_{max}	maximum bending moment
M_y	bending moment at yield limit
M_u	bending moment at ultimate limit
M_W	earthquake magnitude
P	applied axial force
P_o	nominal axial load capacity
Δ_u	ultimate displacement
Δ_y	yield displacement
Δ_p	plastic displacement
ε_{max}	concrete strain at peak stress
ε_{sy}	yield strain of steel reinforcing

ε_{su}	ultimate strain of steel reinforcing
φ	Curvature
φ_{cr}	cracking curvature
φ_y	yield curvature
φ_u	ultimate curvature
θ	rotation
θ_e	elastic rotation
θ_p	plastic rotation
θ_t	total rotation
ρ	mass density
E	modulus of elasticity
ν	poisson's ratio
α	shape factor
PGA	peak ground acceleration
PGV	peak ground velocity
PGD	peak ground displacement